Engineering Science & Technology
https://ojs.wiserpub.com/index.php/EST/

Research Article

Nonlinear Oscillations and Buckling Prediction for Shallow Convex Shells

V. A. Grachev, Yu. S. Neustadt*

Academy of Building and Architecture, Samara State Technical University, 194 Molodogvardeiskaya Str, Samara, 443001, Russia
E-mail: neustadt99@mail.ru

Received: 1 July 2023; **Revised:** 4 August 2023; **Accepted:** 23 August 2023

Abstract: Since 2010, the testing of thin-walled shallow shells has revealed that the ultimate internal stresses, under which the shells lose their stability (collapse), appear to be lower than those predicted by the buckling theory used in American and European standards. The existing norms are based on the static theory of shallow shells proposed in 1930, with stable solutions for thin-walled structures within the nonlinear theory. These stable solutions differ significantly from the forms of equilibrium common to small initial loads. The minimum load, under which an alternative form of equilibrium exists, was used as the ultimate load. In the 1970s, this approach was proved to be unacceptable for complex loadings that were not a part of the real world in the past but are now the case with thinner products operated under complex conditions. Therefore, the initial theories on bearing capacity evaluations must be revisited. The new theory could be built on the basis of recent mathematical results establishing that the estimates made by two schemes (three-dimensional dynamic theory of elasticity and dynamic theory of shallow convex shells) were asymptotically close. Green's special function is introduced to convert the Foppl-von Karman system into a resolving integro-differential equation. The obtained nonlinear equation allows for the separation of variables and has numerous time-periodic solutions that satisfy the Duffing equation with a "soft spring". Numerical analysis enables determination of the amplitude and period of oscillations depending on the properties of Green's function. This paper reviews an experimental setup in which oscillations are generated with the probing load directed normally to the surface of the shell. The experimental measurements of the resonance displacements as a function of coordinates and time enable the calculation of the safety factor for the bearing capacity of the structure using a non-destructive method under operating conditions.

***Keywords*:** dynamic equations for shallow shells, nonlinear oscillations, Green's tensor, Duffing equation, safety factor, buckling prediction

Nomenclature

S_0, S_1	External and internal surfaces of the thin shell
S	Middle surface of the thin shell
h	Thickness of the shell
R	Minimum radius of the curvature of the middle surface of the shell
α, β	Designations of points on the middle surface

DOI: https://doi.org/10.37256/est.5120243316

α_1, α_2	Curvilinear coordinates of the middle surface
A_1, A_2	Coefficients of the first quadratic form for the middle surface
R_1, R_2	Curvature radii of the coordinate lines of the middle surface
x_i	Cartesian coordinates of the middle surface points (i = 1, 2, 3)
S_{0i}, S_{1i}	Surfaces virtually different from S_0, S_1
q_i (α_1, α_2)	Load applied to the middle surface
w_1, w_2	Components of displacements of the middle surface points along α_1 and α_2
w	Displacement along the normal to the middle surface
w^0	Initial imperfections of the middle surface
m_u, m_l	Coefficients of the highest and lowest critical loads within the von Karman-Tsien equations
W	Elastic energy of the shell
ε_{ij}	Strain tensor of the shell
E_{ijkp}	Elastic modulus tensor of the anisotropic shell
E	Elastic modulus of the isotropic shell
ρ	Density of the isotropic shell
N_{11}, N_{22}	Normal forces within the shell along the axes α_1 and α_2
N_{12}	Shear forces in the tangent plane of the shell
Φ	Stress function that defines forces in the tangent plane
$G(\alpha, \beta)$	Green's modified function
$w(\alpha)$	Amplitude displacements of the points during periodic oscillations of the shell
$T(t)$	Duffing periodic functions
$u_0(\alpha)$	Amplitude under the trial load during the testing of the shell
s^*	Material deformation when the yield strength is reached
n_*	Safety factor

1. Introduction

The buckling problems for thin elastic shells have become relevant again [1], [2]. Issues arose during the testing of the thin aviation shells made of high-strength alloys. The main contradiction is as follows: the ultimate internal stresses, under which the shells lose their stability (collapse) (when the load that is proportionally increased over time is slowly applied), appear to be lower than those predicted by the modern theory used in American and European standards. Let us review this in detail.

A shell is a three-dimensional body limited with surfaces S_0, S_1. The distance between these surfaces does not exceed h (the thickness of the shell). The shell is thin; $h/R << 1$, where R is the minimum radius of the curvature of any surface S_0, S_1. Points x_i of smooth surfaces S_0 and S_1 are endowed curvilinear coordinates α_1, α_2 such that in the fixed 3D Cartesian reference system, $x_i = \psi_i(\alpha_1, \alpha_2)$, where ψ_i is a function of two variables consisting continuous partial derivates $D^n(\psi_i)$ with respect to α_1, α_2 through the third order. Therefore, functions ψ_i are limited by the following norm:

$$\|\psi_i\| = \sum_{0 \le n \le 3} \max D^n(\psi_i), D^n(\psi_i) = \frac{\partial^{\beta_1+\beta_2}(\psi_i)}{\partial^{\beta_1}(\alpha_1)\partial^{\beta_2}(\alpha_2)}, 0 \le \beta_1 + \beta_2 \le 3, D^0(\psi_i) = \psi_i$$

Along with the surfaces S_0, S_1, let us review various closely shaped shells with surfaces $S_{0i} = S_0 + \delta S_{0i}$, $S_{1i} = S_1 + \delta S_{1i}$. For the Cartesian point coordinates of surfaces S_{0i}, S_{1i1}, $x_{0i} = x_i + \delta\psi_i$ exists, where $\delta\psi_i$ are smooth functions that are small with respect to the norm. They correspond to the permissible errors (defects) when the shells are made.

The bearing capacity of the shells is tested in two ways. In the first case, the vector function of load $q_i(\alpha_1, \alpha_2)$, causing elastic internal stresses, is applied to surfaces S_0, S_1 at the initial time. Then, the load is increased with the slow (starting from 1) monotonic growth of variable m in equation $Q_i(\alpha_1, \alpha_2) = q_i(\alpha_1, \alpha_2)m$.

When m changes, the shell is deformed, and as long as $1 \le m < m_u$, the coordinates of the x_i points of surfaces S_0, S_1 are defined uniquely. When the m_u value is reached, the equilibrium is bifurcated: the coordinates of x_i increase almost

infinitely. Bifurcation drastically changes the shape of the shell and is accompanied with the "sonic slamming". The parameter m_u is called the highest critical value of the load.

In the second case, surfaces S_{0i}, S_{1i} are loaded with the same load, $Q_i(\alpha_1, \alpha_2)$. As long as $m < m_l$, the deformations of the shells with imperfections δS_{0i}, δS_{1i} continuously grow. When $m = m_l$, geometric shapes are bifurcated, and large irreversible deformations appear on the specimens of the shells "most vulnerable" to buckling failure. The most sensitive are the pieces with norms $\|\delta\psi_i\|$ that differ from the corresponding expressions $\|x_i\|$ for flawless shells as much as possible. The number m_l is called the lowest critical value of the load. $m_l \ll m_u$ is essential for ideally made smooth shells (represented as analytic functions in Cartesian coordinates). Therefore, until recently, the technical standards in all countries referred to the lowest value of m_l [3] to assign ultimate loads. This approach was supported by the theoretical analysis of shell stability that has a long history as well as the fact that almost no flawless shells exist.

The main outcomes of the shell stability theory are as follows. Under any approach, a three-dimensional problem of elastic deformation is reduced to a two-dimensional problem [4], [5]. The middle surface, $S = (S_0 + S_1)/2$, is defined in such a way that any point of the thin shell is described with curvilinear coordinates α_1, α_2 of that surface, and the third coordinate, α_3, counted normally to S at point (α_1, α_2). The external stress is considered to be applied to S. During the loading (on vector $w_i = x_i^+ - x_i$), the points with initial coordinates x_i move to position x_i^+ in accordance with the Kirchhoff-Love hypothesis: the points that lay on the normal to S before the application of forces are on the normal of formed surface S_+ after the force action. The α_3 does not change. The deformation of the ideally shaped shells is studied when $m < m_u$ on the assumption of small displacements based on the energy minimum principle $\Pi(w_i, q_i) = W + A$, where the second member on the right is the work performed by the external forces applied to middle surface $A = \int_S q_i w_i dS$, whereas the first member - $W = \frac{1}{2}\int_D E_{ijkp}\varepsilon_{ij}\varepsilon_{kp}dx$ - is the elastic internal energy of the three-dimensional continuum of the shell. Here, D denotes the volume of the shell, dx denotes the element of the volume, dS denotes the differential of surface area S, E_{ijkp} denotes the elastic modulus tensor, and ε_{ij}, denotes the strain tensor dependent on vector w_i. The formulas for W hold the squares of the first- and second-order derivatives of functions w_i, whereas the equations for A hold only displacements w_i. In this case, only one solution to the problem of shell deformation exists, and internal stresses σ_i are single-valued. The highest critical value of m_u is postulated by Euler's criterion: static load $m_u q_i$ causes additional elastic movements w_i^+ and stresses σ_i^+ that are balanced with internal stresses σ_i during displacements w_i^+. The minimum principle Π related to movements w_i^+ leads to the linear problem of eigenvalues; the minimum eigenvalue defines parameter m_u.

Another method is typically used to calculate m_l. The minimum of function $\Pi(w_i, q_i)$ is searched, but in the equations for W, tensor $\varepsilon_{ij}(w_i)$ is considered in a non-linear form by introducing the covariant derivative of the displacement vector w_i - $\varepsilon_{ij} = \frac{1}{2}(\nabla_i w_j + \nabla_j w_i - \nabla_i w_k \nabla_j w^k)$. Furthermore, the Kirchhoff-Love hypothesis is assumed to be met, and no dynamic effects are assumed to occur. Transitioning of problem $\min\Pi(w_i, q_i)$ to differential equations results in a nonlinear system with a non-unique solution. Stable and unstable branches appear. Number m_l is calculated under the following condition: m_l is a minimum value when a stable solution exists for the nonlinear system corresponding to $\min\Pi(w_i, q_i)$. Notably, the numerical analysis of the system is considerably complex. Therefore, many authors simplified the equations, neglecting the small members within the problems for the smooth shells that could often be seen in practice. The most well-known variation is related to the convex shallow shells and belongs to von Karman and Tsien [6], who applied Foppl's ideas [7] to the shells. Thus, it is often called the Foppl-von Karman variation. The fundamental addition was made by Koiter [8]. When calculating m_l for the smooth shells, the values of w_i are large (approximately 10-fold width). Experimental verification of this result is difficult because ideally shaped shells cannot be made. If we review the shells with initial imperfections w_i^0, then after the calculations, we obtain values m_l^0 that do not considerably differ from m_l, and "visible displacements" $(w_i - w_i^0)$ can be practically observed when testing the shells with surfaces $S + \delta S$. Therefore, the real values of m_l are obtained based on the analysis of the Foppl-von Karman equations applied to the shells with initial defects δS. To 1930, calculations by many authors are related to the most commonly encountered shells, that is, smooth surfaces loaded with a smooth load. In these cases, the theoretical and experimental results were similar for the lowest critical parameter, m_l. However, during the last 20 years, stronger and thinner shells have been used, whereas the loads are not as smooth as they were in the past. Testing shows that the values of m_l that are significantly smaller than those calculated per the Foppl-von Karman model. This was theoretically predicted in the past because a unique solution does not exist for the static Foppl-von Karman system that is equal to m_l

= 0 for a non-zero load q_i (the specific example is given in [9]). Recently, a close result has been numerically obtained by Hutchinson [10] for a spherical shell loaded with concentrated forces. Clearly, the static Foppl-von Karman equations require adjustments. Numerous attempts have been made to update the static and dynamic equations of the shell theory based on the analysis of the small parameters present in the system. The main small parameters of the theory are as follows: $\varepsilon_1 = h/L$, $\varepsilon_2 = L/R$, where L denotes the size of the shell and R denotes the smallest radius of the curvature for one of the coordinate lines. Expanding three-dimensional dynamic equations within the theory of elasticity in powers of polynomials $\varepsilon_1^{p_1}\varepsilon_2^{p_2}$, different updates have been made to the theory of shallow shells [11], [12]. Notably, in the case of any updates, when $p_1 + p_2 \leq 6$, the systems generated are structurally similar to those of the Foppl-von Karman dynamic equations. Based on the applicable classification, the system of nonlinear partial differential equations is of the hyperbolic type. Two boundary value problems can be set: Cauchy and mixed boundary value problems. When solving the Cauchy problem, a surface is selected within the unbounded space where the displacements and velocities are set at the initial moment, and solitary waves (solitons) are detected that are spread almost undistorted [13]. This fact can be used to predict buckling if the soliton is artificially reproduced under loads lower than the critical loads [14]. However, this approach is difficult to implement because the experimental area of the soliton spread is considerably large. Another shortcoming of the asymptotic expansion with respect to the small parameters is the lack of strong evidence to prove process convergence; only the reasoning on the "physical level of rigor" exists. Accurate mathematical results have been obtained relatively recently [15], [16]. The behavior of vector $w_i(x)$, defined within the three-dimensional volume of shell $x \in D$, is studied during time t from interval H as an object of Sobolev space $M = L_2(H) \times W_2^1(D)$. The norm within this space is denoted as $||w_i||_M$. The shell is convex and thin; $\varepsilon = h/R << 1$. The following has been proven: if within space M, a solution exists to the dynamic problem of the theory of elasticity, then under asymptotic aspiration $\varepsilon \to 0$ in terms of Γ- convergence [17], [18], it differs from the solution to the problem for the shell (with middle surface S), calculated per the Foppl-von Karman equations, by no more than $\varepsilon a||w_i||_M$, where $a = const$. The required theorem of existence is proven in [19]-[21]. Hence, the obtained assessment can be used to analyze the behavior of the shells at large dynamic displacements when deformations that are unacceptable for the normal operation exist. Therefore, the following mixed boundary value problem can be set for the Foppl-von Karman system: let the subarea of shell $S_l \subset S$ be loaded with time t periodic load $q_i(S_l)cos\omega t$, $\omega = const$, oriented normally to the surface. The boundary of domain S is fixed, and the amplitude of the external loading is chosen such that when forces $q_i(S_l)$ are applied statically, the internal stresses inside the shell are significantly lower than the yield strength of the material irrespective of frequency ω. By conducting an experiment corresponding to the described problem, let us determine resonance ω^* and the amplitude of the oscillations of shell points $w_i^*(x_i, q_i, \sigma_{oi})$. Here σ_{oi} is the level of internal preliminary stresses during testing. Knowing function $w_i^*(x_i, q_i, \sigma_{oi})$, we can make a displacement picture for shell $w_i^*(x_i, q_i, n\sigma_{oi})$ under stresses $n\sigma_{oi}$ and specify at the value of n at which deformations become unacceptable. Henceforth, the goal is to justify the statement in detail. At first, the well-known Foppl-von Karman dynamic equations describing nonlinear deformations of shallow shells are introduced (detailed description of how these equations are derived, including mechanical and mathematical assumptions, can be found in the Appendix). It is demonstrated that the derived system is converted into one integro-differential equation using Green's modified tensor. Then, based on this, the forced nonlinear waves are studied within the shallow shells loaded with the time-period load applied normally to the surface. The analysis of the oscillations enables an experimental setup that assists in evaluating the safety factor for the shell using a non-destructive method under operating conditions.

2. Conversion of Foppl-von Karman dynamic equations for shallow shells into the integro-differential equation

Studies of 3D thin solids involve the analysis of 2D middle surfaces S defined with local orthogonal coordinates α_1, α_2. For shallow shells, the coefficients of the first quadratic form are as follows: $A_1 = A_2 = 1$. The direction of the normal to surface S is designated as α_3. Curvatures k_1, k_2 of the coordinate lines on surface S are expressed in terms of the radii of the curvatures, $k_1 = 1/R_1$, $k_2 = 1/R_2$. The displacements of the middle surface points towards local coordinates α_1, α_2, α_3 are designated as w_1, w_2, w. Within the Foppl-von Karman equations used to calculate lengthenings of the middle surface, there are linear terms w_1, w_2 and quadratic term w, whereas accelerations in plane S are neglected. Taking into

account elastic stress-strain relations in the tangent plane, the equation of the strain continuity is obtained as

$$\frac{1}{Eh}\nabla^4\Phi = -\frac{1}{2}(L(w,w) - \nabla_k^2(w)) \tag{1}$$

Stress function Φ is related to momentless forces within the shell, similar to the plate

$$N_{11} = \frac{\partial^2\Phi}{\partial\alpha_2^2},\ N_{22} = \frac{\partial^2\Phi}{\partial\alpha_1^2},\ N_{12} = -\frac{\partial^2\Phi}{\partial\alpha_1\partial\alpha_2}$$

In Equation (1), E is the elastic modulus and h is the thickness of the shell. The operators in Equation (1) take the following form

$$L(w,u) = \frac{\partial^2 w}{\partial\alpha_1^2}\frac{\partial^2 u}{\partial\alpha_1^2} + \frac{\partial^2 w}{\partial\alpha_2^2}\frac{\partial^2 u}{\partial\alpha_2^2} - 2\frac{\partial^2 w}{\partial\alpha_1\partial\alpha_2}\frac{\partial^2 u}{\partial\alpha_1\partial\alpha_2} \tag{2}$$

$$\nabla_k w = k_2\frac{\partial^2 w}{\partial\alpha_1^2} + k_1\frac{\partial^2 w}{\partial\alpha_2^2} \tag{3}$$

$$\nabla^2 = \frac{1}{A_1A_2}\left(\frac{\partial}{\partial\alpha_1}\left(\frac{A_2}{A_1}\frac{\partial}{\partial\alpha_1}\right) + \frac{\partial}{\partial\alpha_2}\left(\frac{A_1}{A_2}\frac{\partial}{\partial\alpha_2}\right)\right) \tag{4}$$

The second differential equation defines the dynamic displacement of the shell points towards α_3

$$\rho h\frac{\partial^2 w}{\partial t^2} + D\nabla^4 w - L(w,\Phi) - \nabla_k\Phi + q = 0 \tag{5}$$

Letter t denotes time, whereas ρ denotes the density of the shell material, and q is a surface load in points S in the direction of the normal; $D = Eh^3/12(1-\mu^2)$, μ is Poisson's ratio. Equations (1) and (5) form a full system enabling to the study of the movement of shallow shells when one component of displacement vector w exceeds the others. Functions w, Φ are defined within a simply connected domain S_L with boundary L, where four conditions are met:

$$w(L) = \frac{\partial w}{\partial n}(L) = 0,\ N_n(L) = \frac{\partial^2\Phi}{\partial\alpha_s^2},\ N_s(L) = \frac{\partial^2\Phi}{\partial\alpha_n\partial\alpha_s} \tag{6}$$

Functions $N_n(L)$, $N_s(L)$ represent momentless stresses, and n, s denote the directions of the normal and tangent, respectively, to line L.

Equations (1) and (5) with boundary conditions (6) can be converted into one integro-differential equation concerning function $w(\alpha, t)$ if Green's function $G(\alpha, \beta)$ is first constructed for the biharmonic equation with two boundary conditions:

$$\frac{1}{Eh}\nabla^4 G(\alpha,\beta) = -\delta(\beta),\ \frac{\partial^2 G(\alpha,\beta)}{\partial\alpha_s^2} = N_n(L),\ \frac{\partial^2 G(\alpha,\beta)}{\partial\alpha_n\partial\alpha_s} = N_s(L) \tag{7}$$

Here, α, β denote various arbitrary internal points of surface S_L, and $\delta(\beta)$ represents the Dirac function at point

β. Operator ∇^4 is calculated at point α. The Green tensor is constructed in the following order. First, function $\varphi(\alpha)$ is determined by the following conditions:

$$\nabla^4\phi(\alpha)=0,\ \frac{\partial^2\phi(\alpha)}{\partial\alpha_s^2}=N_n(L),\ \frac{\partial^2\phi(\alpha)}{\partial\alpha_n\partial\alpha_s}=N_s(L) \tag{8}$$

This function exists because it solves the plane elasticity problem with known stresses on contour L [24]. Let us determine the value of the function found on contour L--$\varphi(L)$ and the value of normal derivative $\frac{\partial\phi}{\partial n}(L)$. Next, we calculate the boundary values of the functions on contour L

$$r^2\ln r(\alpha,L)=\phi_1(\alpha,L),\ \frac{\partial(r^2\ln r(\alpha,L)}{\partial n}=\frac{\partial\phi_1}{\partial n}(L) \tag{9}$$

Here $r(\alpha, \beta)$ is the Cartesian distance between points α, β. Let us construct function $\varphi_2(\alpha)$ using the following conditions:

$$\nabla^4\phi_2(\alpha)=0,\ \phi_2(L)=\phi(L)-\phi_1(\alpha,L),\ \frac{\partial\phi_2}{\partial n}(L)=\frac{\partial\phi}{\partial n}(L)-\frac{\partial\phi_1}{\partial n}(L) \tag{10}$$

Because $r(\alpha, \beta)$ is a biharmonic function with respect to any variable α, β, equality $G(\alpha, \beta) = r^2\ln r(\alpha, \beta) + \varphi_2(\alpha)$ occurs. The properties of the introduced Green's function enable us to re-write equality (1) as follows:

$$\Phi(w,\alpha)=\frac{1}{2}\iint_{S_L}G(\alpha,\beta)(L(w(\beta),w(\beta))-\nabla_k^2w(\beta))A_1A_2d\beta_1d\beta_2 \tag{11}$$

Substituting (11) into (5), we obtain the following integro-differential equation for further analysis.

$$\rho h\frac{\partial^2w(\alpha,t)}{\partial t^2}+D\nabla^4w(\alpha,t)-L(w(\alpha,t),\Phi(\alpha,t))-\nabla_k\Phi(\alpha,t)+q(\alpha,t)=0 \tag{12}$$

3. Deformation of shallow shells under time-periodic exposure

Let us ensure that homogeneous equation (12) allows for creating "standing waves". In other words, the separation of variables is possible, and the following solution exists.

$$w(\alpha,t)=T(t)\times u(\alpha) \tag{13}$$

Now, we substitute (13) into (12) (in case of $q(\alpha, t) = 0$), multiply the calculated amount by $u(\alpha)$, and integrate the result with respect to surface S_L. Thus,

$$a_0\frac{d^2T}{dt^2}+a_1T+a_2T^2-a_3T^3=0 \tag{14}$$

The following designations are introduced:

$$a_0 = \rho h \iint_{S_L} u^2(\alpha) dS_\alpha,\ dS_\alpha = A_1(\alpha)A_2(\alpha)d\alpha_1 d\alpha_2,\ dS_\beta = A_1(\beta)A_2(\beta)d\beta_1 d\beta_2$$

$$a_1 = D\iint_{S_L} u(\alpha)\times\nabla^4(\alpha)dS_\alpha - \frac{1}{2}\iint_{S_L} u(\alpha)\times(\iint_{S_L}\nabla_k^2 G(\alpha,\beta)u(\beta)dS_\beta)dS_\alpha$$

$$a_2 = \frac{1}{2}\iint_{S_L} u(\alpha)\times(L(u(\alpha),(\iint_{S_L} G(\alpha,\beta)\nabla_k^2 u(\beta)dS_\beta))dS_\alpha$$

$$a_3 = \frac{1}{4}\iint_{S_L} u(\alpha)\times(L(u(\alpha),(\iint_{S_L} G(\alpha,\beta)(L(u(\beta),u(\beta))dS_\varphi))dS_\alpha \tag{15}$$

Function $u(\alpha)$ is obtained from Sobolev space $W_2^2(S_L)$; the second and third derivatives can jump on internal lines L_g. Therefore, the first integral in coefficient a_1 is re-written in the form of $D\iint_{S_L} u(\alpha)\times\nabla^4(\alpha)dS_\alpha = \Pi + \int_{L_g} M_g \frac{\partial u}{\partial n} dl_g + \int_{L_g} Q_g u dl_g$, where n denotes the normal to curvature L_g; functions M_g, Q_g are expressed in terms of derivative jumps $u(\alpha)$ (designated with straight lines) by the following equations:

$$Q_g = D\left|\frac{\partial}{\partial n}(\nabla^2 u)\right|,\ M_g = D\left|\frac{\partial^2 u}{\partial n^2}\right| \tag{16}$$

Potential energy Π is defined as follows:

$$\Pi = \frac{D}{2}\iint_{S_L}((\frac{\partial^2 u}{\partial\alpha_1^2}+\frac{\partial^2 u}{\partial\alpha_2^2})^2 + 2(1-\mu)((\frac{\partial^2 u}{\partial\alpha_1\partial\alpha_2})^2 - \frac{\partial^2 u}{\partial\alpha_1^2}\frac{\partial^2 u}{\partial\alpha_2^2}))dS_\alpha$$

Equation (14) has been thoroughly studied [25]-[27]. It simulates the Duffing oscillator with the "soft spring". The force and potential functions of the oscillator are as follows:

$$f(T) = a_1 T + a_2 T^2 - a_3 T^3,\ V(T) = \frac{1}{2}a_1 T^2 + \frac{1}{3}a_2 T^3 - \frac{1}{4}a_3 T^4$$

The graphs of functions $f(T)$, $V(T)$ are shown in Figure 1(a, b). Figure 1(c) shows the integral curves of Equation (14) on the phase plane $(T, \dot{T} = \frac{dT}{dt})$.

The internal area, D_p, of the phase plane between separatrixes is filled with periodic curvatures around equilibrium point $T = \dot{T} = 0$. The oscillation period (unlike the linear case) is a function of amplitude T_a: the closer to the separatrix, the larger the period is; on the separatrix, it is infinite. Forced vibrations caused by a load such as $q(\alpha, t) = b(\alpha)\cos\omega t$ with constant frequency ω can be studied. The described problem is equivalent to determining periodic solutions to the following equation.

$$a_0\frac{d^2T}{dt^2} + a_1 T + a_2 T^2 - a_3 T^3 = b_0\cos t\omega,\ b_0 = \iint_{S_L} b(\alpha)u(\alpha)dS_\alpha \tag{17}$$

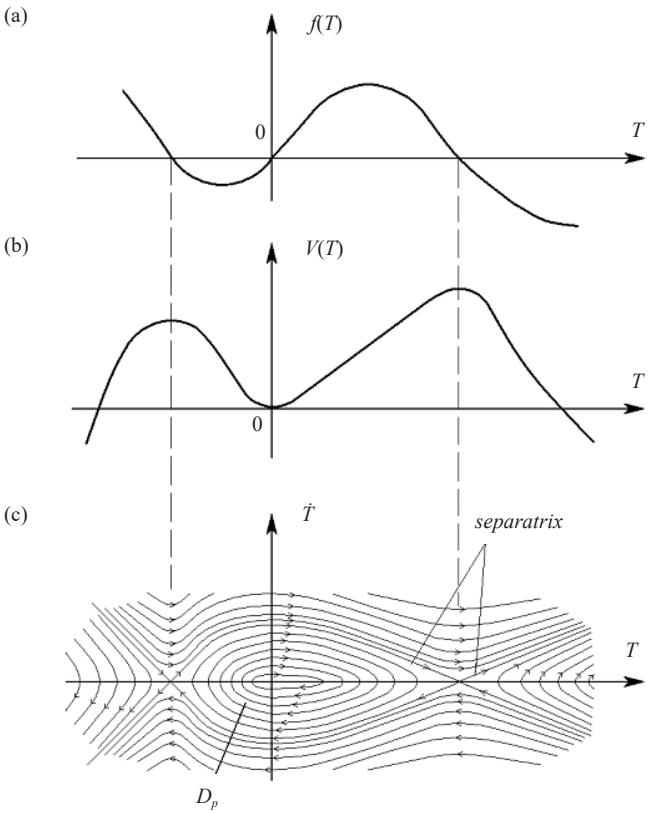

Figure 1. a) Force action $f(T)$ from the Duffing equation against time function T, b) Potential $V(T)$, related to the Duffing equation, against time function T, and c) Phase plane of solutions to the Duffing equation with the "soft spring"; the area of periodic solutions is denoted as D_p

As proven, a nonlinear resonance can occur in a non-autonomous system at some frequency ω_0, whereas the dynamic displacement of the shell is considerably bigger than movements from statical load $b(\alpha)$. The solutions to Equation (17) within the resonance area have a complex multiform structure. The stroboscopic Poincare mapping [28], [29] is used to extract single-valued solutions. Based on this, we rewrite (17) as an autonomous system in the three-dimensional space as follows:

$$\frac{dT}{dt} = Y,\ a_0 \frac{dY}{dt} = -a_1 T - a_2 T^2 + a_3 T^3 - b_0 \cos Z,\ \frac{dZ}{dt} = \omega \tag{18}$$

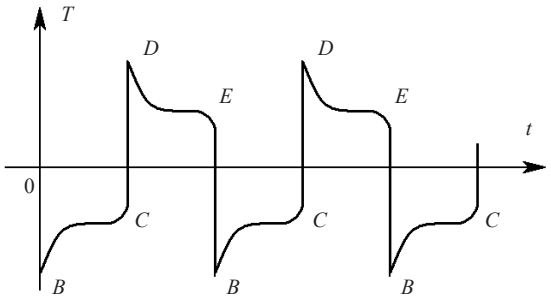

Figure 2. The graph of periodic function T from the Duffing equation against time t when approaching the separatrix

The stroboscopic mapping of function T over the period of oscillations $\Delta = 1/\omega$ is denoted with the same letter as shown in Figure 2.

The main features of nonlinear resonance must be discontinuities of function T during each period of oscillation. The value of the oscillation period within the critical area close to the separatrix can be assessed analytically. The motion becomes relaxational [30] owing to the inclusion of damping into the second homogeneous equation in (18) with coefficient c.

$$a_0 \frac{dY}{dt} = -a_1 T - a_2 T^2 + a_3 T^3 - cY$$

Small parameter a_0 (for the thin shell) enables the integration of equation $c\frac{dT}{dt} = -a_1 T - a_2 T^2 + a_3 T^3 = f(T)$ (Figure 3). Consequently, $\Delta = \int_{BC+DE} cdT / f(T)$. Only numerical assessment of the period and amplitude of the oscillations within domain D_p per Figure 1(c) is possible.

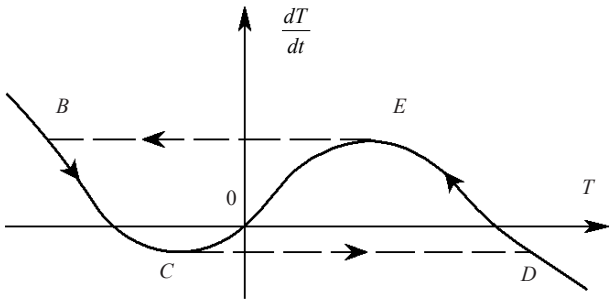

Figure 3. Relaxation periodic oscillations (curvature *BCDE*) on the phase plane for the Duffing equation

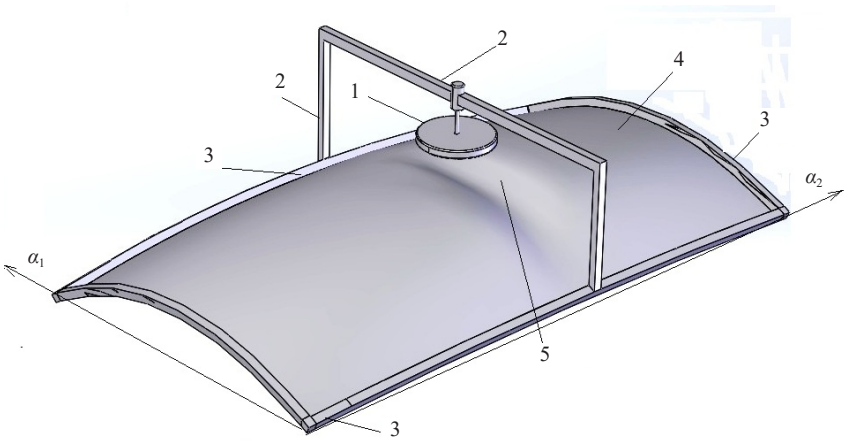

1-oscillation excitation coil
2-coil attachment to the strengthening contour
3-strengthening contour of the shell
4-surface of the shell
5-"buckling" dent generated under periodic oscillations

Figure 4. Safety factors measuring machine

4. Experiments that allow for the assessment of safety factors for the thin shallow shells

The buckling of the shallow shells is followed by the formation of large dents on the middle surface. Dents L_d are at least one-third the size of shell L. The movement of the dent can be observed if a magnetic coil that causes oscillations per law $q(\alpha, t) = b_0(\alpha)\cos\omega t$ is placed above the shell (Figure 4). Value $b_0(\alpha)$ is adjusted such that the stresses initiated by the static application of this load together with the momentless stresses of the main loading are nowhere near the yield strength of the material.

When changing the exciting frequency ω, the nonlinear resonance occurs at some value of ω_0. Let us measure the maximum displacement of shell $u_0(\alpha)$ and period of resonance oscillations $\Delta_0 = 1/\omega_0$. Momentless forces acting in the shell under normal operation are denoted as $N_n(\alpha)$, $N_s(\alpha)$.

$$N_{0n}(\alpha) = p_1 N_n(\alpha),\ N_{0s}(\alpha) = p_2 N_s(\alpha) \tag{19}$$

Values N_n, N_s are generally known, and numbers p_1, p_2 can be obtained based on the numerical analysis of equations (18)-(21) because $u_0(\alpha)$ and ω_0 are experimentally determined. The deformations and curvatures of the shell surface that occur during testing can be estimated based on the linear analysis within the momentless theory of the shells [22].

Next, the following problem can be set: how much should the external load (or internal forces $N_{0n}(\alpha)$, $N_{0s}(\alpha)$) be increased to cause irreversible plastic yield (bearing capacity failure) in the shell. In other words, at what number n_*, the forces on the contour L

$$N_{*0n}(L) = n_* p_1 N_n(L),\ N_{*0s}(L) = n_* p_1 N_s(L) \tag{20}$$

initiate irreversible deformations if a periodic load with small amplitude $b_0(\alpha)$ is applied to the shell.

Let us review a situation in which the excitement with probing load $b_0(\alpha)$ results in additional displacements $u_0(\alpha)$ that can be accurately measured. The experiments demonstrate that in this case, the displacements that cause buckling can be roughly described using the formula $K_0 u_0(\alpha)$.

The irreversible displacements are typically described in two ways. If function $u(\alpha)$ is differentiable up to the third order, the irreversible deformations are related to the stresses responsible for the plasticity of the material. Because the stresses are proportional to the bending moments M_{ij}, they can be considered proportional to the norm of the second-order derivatives of motion $m_1 = \sum_{i,J=1}^{2} \left| \frac{\partial^2 (u(\alpha)}{\partial \alpha_i \partial \alpha_2} \right|$. If the second-order derivatives discontinue on some lines L_g, the ultimate stresses are proportional to the value m_2, that is, the function jump $m_2 = \sum_{i,J=1}^{2} \left| \frac{\partial^2 (u(\alpha)}{\partial \alpha_i \partial \alpha_2} \right|$. Let us denote values m_1, m_2 related to function $u_0(\alpha)$ as m_1^0, m_2^0. For the differentiable function $u_0(\alpha)$, we obtain $K_0 = s_1^*/m_1^0$, where s_1^* is the material deformation when the yield strength is reached. If function $u_0(\alpha)$ is discontinuous, then $K_0 = s_2^*/m_2^0$, where s_2^* is a jump of the deformation within the yield-point phenomenon.

To determine n_*, the following calculation method can be proposed. First, let us calculate the coefficients of equation (14) per formula (15) at different values of two parameters: $r > 1$ (in the equations for forces $N_{rn}(\alpha) = rp_1 N_n(\alpha)$, $N_{rs}(\alpha) = rp_2 N_s(\alpha)$) and k represented with possible displacement $u_k = ku_0(\alpha)$, $1 < k \le K_0$. Next, we determine the periodic solution to equation (14) within domain D, as shown in Figure 4, with amplitude $T_a(k, r)$ that is a function of two parameters k, r. Owing to representation (17), the buckling (bearing capacity failure) is defined by the following conditions:

$$n_* = \inf r,\ T_a(k, r)k = K_0 \tag{21}$$

Let us now highlight the essential features of the proposed method. Experimental function $u_0(\alpha)$ must ensure nonlinear oscillations, that is, discontinuities of functions T (Figure 2) visible on the graph, under a small trial load at

resonance frequency ω_0. Then, having overcome some calculational complexity [28], we manage to determine a real coefficient of the safety factor, n_*. If the resonance function T is continuous, the safety factor can be considered sufficient for the normal operation in the future.

5. Conclusion

The main outcome of this study is that, for the convex shallow shells, bucking is assessed based on the dynamic analysis of resolving integro-differential equation (16). The obtained equation is an effect of the mathematical achievements in the asymptotic justification of the Foppl-von Karman model within the nonlinear theory of elasticity [31] and prediction of dynamic chaos under ultimate loads [25], [32]. The numerical analysis can be significantly simplified if the results of the experiments are used with the shell being tested under periodic load. This paper includes a conceptual scheme of the experimental setup and the methods to calculate the safety factor. Thus, the suggested approach generalizes the analysis for the buckling prognosis, which was earlier for cylindrical shells [33], to arbitrary convex shallow shells.

Conflicts of interest

The authors declare that there are no conflicts of interest regarding the publication of this paper.

References

[1] M. Hilburger, "Developing the Next Generation Shell Buckling Design Factors and Technologies," 53rd AIAA/ASME/ASCE/AHS/ASC Structures, Structural Dynamics and Materials Conference, Honolulu, Hawaii, 2012.

[2] K. K. Yadav, N. L. Cuccia, E. Virot, S. M. Rubinstein, and S. A. Gerasimidis, "Nondestructive technique for the evaluation of thin cylindrical shells' axial buckling capacity," *Journal of Applied Mechanics*, vol. 88, no. 5, pp. 051003, 2021.

[3] F. Royer, J. W. Hutchinson, and S. Pellegrino, "Probing the stability of thin-shell space structures under bending," *International Journal of Solids and Structures*, vol. 257, pp. 111806, 2022.

[4] A. S. Volmir, *Stability of Elastic Systems*. Moscow, Nauka. English Translation: Foreign Technology, Division, Air Force Systems Command. Wright-Patterson Air Force Base, Ohio, 1965.

[5] J. M. T. Thompson, "Advances in shell buckling: Theory and experiments," *International Journal of Bifurcation and Chaos*, vol. 25, no. 1, pp. 1530001, 2015.

[6] Th. von Karman and H. S. Tsien, "The buckling of cylindrical shells under axial compression," *Journal of Aeronautical Sciences*, vol. 8, no. 8, pp. 303-312, 1941.

[7] A. Föppl, *Vorlesungen über technische Mechanik*. Bd. 5, B. G. Teubner, Leipzig, Germany, 1907.

[8] W. Koiter, "Elastic stability and post buckling behavior in nonlinear problems," In Proceedings of the Symposium on Nonlinear Problems, Madison: University of Wisconsin Press, 1963, pp. 257-275.

[9] I. I. Vorovich, *Nonlinear Theory of Shallow Shells*. English Edition edited by L. P. Lebedev. Translated by M. Grinfeld, Springer - Verlag. New York - Berlin- Heidelberg, 1999.

[10] J. W. Hutchinson, "Buckling of spherical shells revisited," *Proceedings of the Royal Society A: Mathematical, Physical and Engineering Sciences*, vol. 472, no. 2195, pp. 20160577, 2016.

[11] R. K. Dodd, J. C. Eilbeck, J. D. Gibbon, and H. C. Morris, *Solitons and Nonlinear Wave Equations*. London Academic Press, 1982.

[12] M. J. Ablowitz and H. Segur, *Solitons and Inverse Scattering Transform (SIAM Studies in Applied Mathematics, No. 4)*. Society for Industrial and Applied Mathematics, Philadrlphia, 1988.

[13] V. V. Kiselev and D. V. Dolgikh, "Non-linear patterns of bends and solitons on surfaces of loaded shells," *Shell Structure: Theory and Applications*, vol. 3, pp. 199-202, 2013.

[14] Y. S. Neustadt and V. A. Grachev, "Buckling prognosis for thin elastic shallow shells," *Zeitschift der Angewande Math. und Physik*, vol. 70, pp. 113, 2019.

[15] M. Lewicka, M. G. Mora, and M. R. Pakzad, "Shell theories arising as low energy Γ-limit of 3d nonlinear

elasticity," *Annali della Scuola Normale Superiore di Pisa - Classe di Scienze*, vol. 9, no. 2, pp. 253-295, 2010.
[16] P. Hornung and I. Velcic, "Derivation of a homogenized von-Kármán shell theory from 3D elasticity," *Annales de l'Institut Henri Poincaré C, Analyse non linéaire*, vol. 32, no. 5, pp. 1039-1070, 2015.
[17] E. De Giorgi and T. Franzoni, "Su un tipo di convergenza variazionale," *Atti della Accademia Nazionale dei Lincei. Classe di Scienze Fisiche, Matematiche e Naturali. Rendiconti*, vol. 58, no. 6, pp. 842-850, 1975.
[18] G. Dal Maso, *An Introduction to Γ-Convergence*. Progress in nonlinear differential equations and their applications, Boston, MA, Birkhauser, 1993.
[19] J. M. Ball, "Convexity conditions and existence theorems in nonlinear elasticity," *Archive for Rational Mechanics and Analysis*, vol. 63, pp. 337-403, 1977.
[20] V. G. Vilke, "Existence and uniqueness theorem for solutions of dynamic problems of the nonlinear theory of elasticity," *Journal of Applied Mathematics and Mechanics*, vol. 44, no. 4, pp. 501-507, 1980.
[21] P. Marcellini, "Existence theorems in nonlinear elasticity," *North-Holland Mathematics Studies*, vol. 129, pp. 241-247, 1986.
[22] V. V. Novozhilov, *Foundations of the Nonlinear Theory of Elasticity*. Rochester-New York: Gray lock Press, 1953.
[23] K. F. Chernyh, *An introduction to Modern Anisotropic Elasticity*. New York (USA) Wallingford (UK), Begell Publishing House, 1998.
[24] N. I. Muskhelishvili, *Some Basic Problems of the Mathematical Theory of Elasticity*. Leyden: Noordhoff International Publishing, 1977.
[25] J. Guckenheimer and P. Holmes, *Nonlinear Oscillations, Dynamical Systems and Bifurcation of Vector Fields*. Berlin: Springer, 1983.
[26] I. Kovacic and M. J. Brennan, Eds., *The Duffing Equation: Nonlinear Oscillators and their Behaviour*. Chichester, UK: Wiley & Sons Ltd., 2011.
[27] T. Kanamaru, "Duffing oscillator," *Scholarpedia* [Online]. Available: http://scholarpedia.org/article/Duffing_oscillator [Accessed Oct. 2014].
[28] D. W. Jordan and P. Smith, *Nonlinear Ordinary Differential Equations-An Introduction for Scientists and Engineers (4th ed.)*. Oxford University Press, 2007.
[29] A. P. Kuznetsov, S. P. Kuznetsov, E. Mosekilde, and N. V. Stankevich, "Generators of quasiperiodic oscillations with three-dimensional phase space," *The European Physical Journal Special Topics*, vol. 222, no. 10, pp. 2391-2398, 2013.
[30] E. F. Mishchenko and N. H. Rozov, *Differential Equations with Small Parameters and Relaxation Oscillations, reprint of the original 1st ed.* New York-London: Springer, 1980.
[31] M. Lewicka, M. G. Mora, and M. R. Pakzad, "The matching property of infinitesimal isometries on elliptic surfaces and elasticity of thin shells," *Archive for Rational Mechanics and Analysis*, vol. 200, no. 3, pp. 1023-1050, 2011.
[32] S. P. Kuznetsov and A. Pikovsky, "Hyperbolic chaos in the phase dynamics of a Q-switched oscillator with delayed nonlinear feedbacks," *Europhysics Letters*, no. 84, pp. 10013, 2008.
[33] Yu. S. Neustadt and V. A. Grachev, "Relaxation oscillations and buckling prognosis for shallow thin shells," *Zeitschrift für angewandte Mathematik und Physik*, vol. 71, no. 4, pp. 142, 2020.

Appendix

Foppl-von Karman dynamic equations for shallow shells

The appendix includes basic postulates used to derive the Foppl-von Karman equations describing nonlinear deformations of thin shells.

It covers shallow shells with middle a surface S described within a fixed Cartesian coordinate system x_i, $i = 1, 2, 3$, with equation $x_3 = \psi(x_1, x_2)$, where ψ is a smooth two-variable function of the third order (Figure A1). Moreover,

$$\frac{\partial x_3}{\partial x_1} << 1, \quad \frac{\partial x_3}{\partial x_2} << 1 \tag{A1}$$

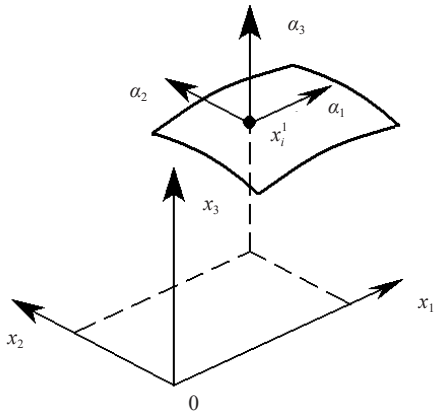

Figure A1. Fragment of the middle surface of the shallow shell with Lagrangian orthogonal coordinates α_1, α_2, α_3. Fixed orthogonal frame of references x_1, x_2, x_3, where point x_i^1 on the middle surface is recorded

This equation enables the introduction of orthogonal coordinates α_1, α_2 for any point of α on surface S such that lines $\alpha_1 = const$, $\alpha_2 = const$ are parallel to $x_1 = const$, $x_2 = const$, and coefficients of the first quadratic form $A_1 = A_2 = 1$. Let the direction of the normal to surface S be α_3 at point α. All internal points on the three-dimensional shell have Lagrangian coordinates α_1, α_2, α_3 (Figure A2). Curvatures k_1, k_2 of the coordinate lines on surface S are expressed in terms of the radii of the curvatures, $k_1 = 1/R_1$, $k_2 = 1/R_2$.

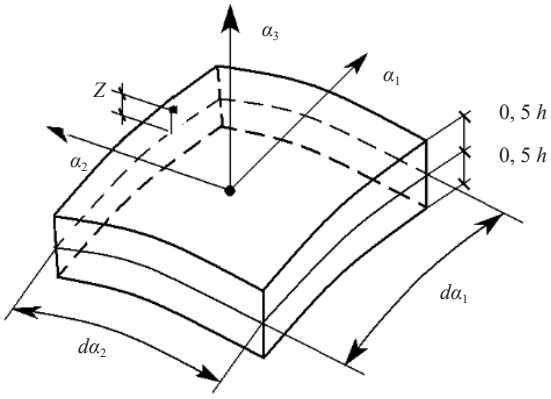

Figure A2. Infinitely small elements of the shell separated along distances $d\alpha_1$, $d\alpha_2$ by surfaces parallel to Cartesian planes $\alpha_1\alpha_3$ и $\alpha_2\alpha_3$. For the element points located on the lateral faces, $z = \alpha_3$

Vector $w_i(\alpha_1, \alpha_2, \alpha_3) = x_i(\alpha_1, \alpha_2, \alpha_3) - x_{0i}(\alpha_1, \alpha_2, \alpha_3)$ describes the movement of any point on the shell from position $x_{0i}(\alpha_1, \alpha_2, \alpha_3)$ to position $x_i(\alpha_1, \alpha_2, \alpha_3)$. Henceforth, we use traditional designations, $\alpha_3 = z$, $w_3 = w$. The points move in accordance with the Kirchhoff-Love hypothesis: the points that initially lay on the normal to the middle surface remain on the normal to deformed surface S (straight-normal hypothesis). The Kirchhoff-Love theory is mechanically equivalent to the assumption in [22], [23] that in flexible bodies, lengthenings and shears are small compared to rotations when determining fiber directions. The metrics of the initial middle surface is written as $ds^2 = g_{ik}d\alpha_i d\alpha_k$, $i, k = 1, 2$, whereas after the deformation, the metrics are $ds_1^2 = g_{ik}^1 d\alpha_i d\alpha_k$, $i, k = 1, 2$. The deformation of the middle surface ε_{ik} is estimated using the following equation:

$$ds_1^2 - ds^2 = \varepsilon_{ik} d\alpha_i d\alpha_k$$

Considering the straight-normal hypothesis, we obtain the following equations:

$$\varepsilon_{11} = \frac{\partial w_1}{\partial \alpha_1} - k_1 w + \frac{1}{2}(\frac{\partial w}{\partial \alpha_1})^2$$

$$\varepsilon_{22} = \frac{\partial w_2}{\partial \alpha_2} - k_2 w + \frac{1}{2}(\frac{\partial w}{\partial \alpha_2})^2$$

$$\varepsilon_{12} = \frac{\partial w_1}{\partial \alpha_2} + \frac{\partial w_2}{\partial \alpha_1} + \frac{\partial w}{\partial \alpha_1} - \frac{\partial w}{\partial \alpha_2} \tag{A2}$$

Excluding component w_1, w_2 from (A2) by differentiation, we obtain the following equation of deformation continuity:

$$\frac{\partial^2 \varepsilon_{11}}{\partial \alpha_2^2} + \frac{\partial^2 \varepsilon_{22}}{\partial \alpha_1^2} - \frac{\partial^2 \varepsilon_{12}}{\partial \alpha_1 \partial \alpha_2} = -\frac{1}{2} L(w, w) - \nabla_k w$$

$$L(w,u) = \frac{\partial^2 w}{\partial \alpha_1^2}\frac{\partial^2 u}{\partial \alpha_1^2} + \frac{\partial^2 w}{\partial \alpha_2^2}\frac{\partial^2 u}{\partial \alpha_2^2} - 2\frac{\partial^2 w}{\partial \alpha_1 \partial \alpha_2}\frac{\partial^2 u}{\partial \alpha_1 \partial \alpha_2}, \ \nabla_k w = k_2 \frac{\partial^2 w}{\partial \alpha_1^2} + k_1 \frac{\partial^2 w}{\partial \alpha_2^2} \tag{A3}$$

The straight-normal hypothesis enables the calculation of the changes in curvatures χ_{11}, χ_{22} on coordinate lines $\alpha_1 = const$, $\alpha_2 = const$ and changes in curvatures of the surface χ_{12}.

$$\chi_{11} = -\frac{1}{A_1}\frac{\partial}{\partial \alpha_1}(\frac{\partial w_1}{R_1} + \frac{1}{A_1}\frac{\partial w}{\partial \alpha_1}) - \frac{1}{A_1 A_2}(\frac{w_2}{R_2} + \frac{1}{A_2}\frac{\partial w}{\partial \alpha_2})\frac{\partial A_1}{\partial \alpha_2}$$

$$\chi_{22} = -\frac{1}{A_2}\frac{\partial}{\partial \alpha_2}(\frac{\partial w_2}{R_2} + \frac{1}{A_2}\frac{\partial w}{\partial \alpha_2}) - \frac{1}{A_1 A_2}(\frac{w_1}{R_1} + \frac{1}{A_1}\frac{\partial w}{\partial \alpha_1})\frac{\partial A_2}{\partial \alpha_1}$$

$$\chi_{12} = -\frac{1}{2}(\frac{A_2}{A_1}\frac{\partial}{\partial \alpha_1}(\frac{w_2}{A_2 R_2} + \frac{1}{A_2^2}\frac{\partial w}{\partial \alpha_2}) + \frac{A_1}{A_2}\frac{\partial}{\partial \alpha_2}(\frac{w_1}{A_1 R_1} + \frac{1}{A_1^2}\frac{\partial w}{\partial \alpha_1})) \tag{A4}$$

The deformations in any point spaced away from the middle surface by z, is written as follows:

$$\varepsilon_{11}(z) = \varepsilon_{11} + z\chi_{11},\ \varepsilon_{22}(z) = \varepsilon_{22} + z\chi_{22},\ \varepsilon_{12}(z) = \varepsilon_{12} + z\chi_{12}$$

For the isotropic elastic shell with Young modulus E and Poisson's ratio μ, the link between the stresses and deformations is as follows:

$$\sigma_{11}(z) = \frac{E}{1-\mu^2}(\varepsilon_{11} + \mu\varepsilon_{22}(z)),\ \sigma_{11}(z) = \frac{E}{1-\mu^2}(\varepsilon_{11} + \mu\varepsilon_{11}(z)),\ \sigma_{12}(z) = \frac{E}{2(1-\mu^2)}\varepsilon_{12}(z) \tag{A5}$$

The stresses affecting the faces of the shell element amount to the resultant line forces and moments (Figure A3) applied to the middle surface S by integration along the coordinate z.

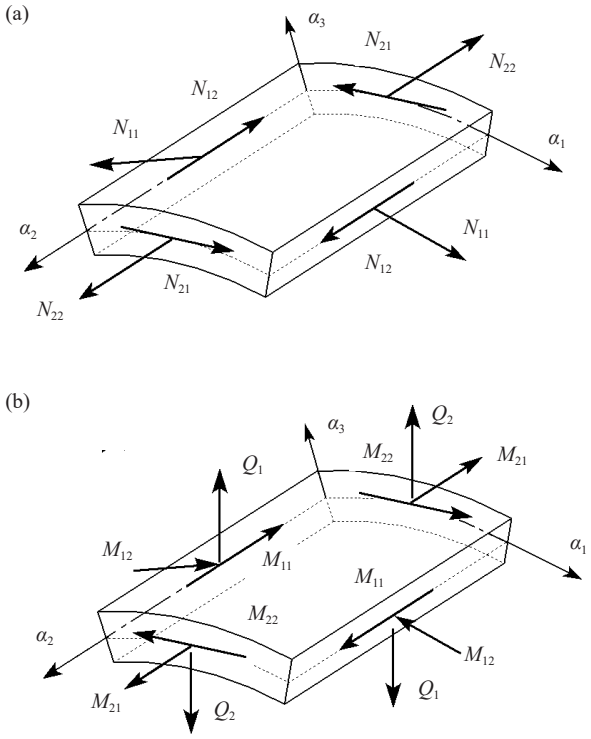

Figure A3. a) Resultant internal forces (N_{11}, N_{22}, $N_{12} = N_{21}$) related to the middle forces and located on plane α_1, α_2. b) Resultant internal lateral forces Q_1, Q_2 of the bending and torsional moments (M_{11}, M_{22}, $M_{12} = M_{21}$) applied to the lateral faces of the shell element

$$N_{11} = \int_{-h/2}^{h/2} \sigma_{11}(z)(1 - \frac{z}{R_2})dz$$

$$M_{11} = \int_{-h/2}^{h/2} \sigma_{11}(z)(1 - \frac{z}{R_2})zdz \tag{A6}$$

The remaining line forces N_{ij}, M_{ij} are estimated similarly by replacing index A1 with index A2. Substituting equation (A5) into (A6), all line forces are as follows:

$$N_{11}=\frac{Eh}{1-\mu^2}(\varepsilon_{11}+\mu\varepsilon_{22}),\ N_{22}=\frac{Eh}{1-\mu^2}(\varepsilon_{22}+\mu\varepsilon_{11}),\ N_{12}=\frac{Eh}{2(1+\mu)}\varepsilon_{12}$$

$$M_{11}=D(\chi_{11}+\mu\chi_{22}),\ M_{22}=D(\chi_{22}+\mu\chi_{11}),\ M_{12}=D(1-\mu)\chi_{12},\ D=\frac{Eh^3}{12(1-\mu^2)} \tag{A7}$$

Values N_{ij}, M_{ij} must satisfy the motion equations. Furthermore, we consider the motion when only normal forces q exist (Figure A3). The equilibrium of the plane forces (first line in (A7)) is equivalent to two equations.

$$\frac{\partial N_{11}}{\partial\alpha_1}+\frac{\partial N_{12}}{\partial\alpha_2}=0,\ \frac{\partial N_{22}}{\partial\alpha_2}+\frac{\partial N_{12}}{\partial\alpha_1}=0 \tag{A8}$$

The existence of stress function Φ with the following properties results from (A8).

$$N_{11}=\frac{\partial^2\Phi}{\partial\alpha_2^2},\ N_{22}=\frac{\partial^2\Phi}{\partial\alpha_1^2},\ N_{12}=-\frac{\partial^2\Phi}{\partial\alpha_1\partial\alpha_2} \tag{A9}$$

Substituting dependences (A9) into the first three equations in (A7), deformations ε_{ij} can be expressed in terms of stresses. Equation (3) is written as follows:

$$\frac{1}{Eh}\nabla^4\Phi=-\frac{1}{2}(L(w,w)-\nabla_k^2(w)) \tag{A10}$$

Symbol ∇^2 denotes Laplace operator $\nabla^2=\frac{1}{A_1A_2}(\frac{\partial}{\partial\alpha_1}(\frac{A_2}{A_1}\frac{\partial}{\partial\alpha_1})+\frac{\partial}{\partial\alpha_2}(\frac{A_1}{A_2}\frac{\partial}{\partial\alpha_2}))$. Another motion equation is obtained based on the analysis of the forces per Figure A3(b). Because the moments of all internal and external forces equal to zero about axes α_1, α_2 (the equality is automatically satisfied about axis α_3), Q_1, Q_2 can be expressed in terms of M_{ij} and their derivatives as follows:

$$Q_1=\frac{1}{A_1A_2}(\frac{\partial(A_1M_{11})}{\partial\alpha_1}+\frac{\partial(A_1M_{12})}{\partial\alpha_2}-M_{12}\frac{\partial A_2}{\partial\alpha_1}+M_{12}\frac{\partial A_1}{\partial\alpha_2})$$

$$Q_2=\frac{1}{A_1A_2}(\frac{\partial(A_2M_{22})}{\partial\alpha_2}+\frac{\partial(A_2M_{12})}{\partial\alpha_1}-M_{12}\frac{\partial A_1}{\partial\alpha_2}+M_{12}\frac{\partial A_2}{\partial\alpha_1}) \tag{A11}$$

When the projections of the internal and inertial forces are equal to zero along the axis α_3, the following equality occurs.

$$\rho h\frac{\partial^2 w}{\partial t^2}+\frac{\partial Q_1}{\partial\alpha_1}+\frac{\partial Q_2}{\partial\alpha_2}+N_{11}(k_1+\frac{\partial^2 w}{\partial\alpha_1^2})+N_{22}(k_2+\frac{\partial^2 w}{\partial\alpha_2^2})+2N_{12}\frac{\partial^2 w}{\partial\alpha_1\partial\alpha_2}+q=0 \tag{A12}$$

Considering (A2), (A4), (A7), and (A11), we obtain the main equation of the Foppl-von Karman system as follows:

$$\rho h\frac{\partial^2 w}{\partial t^2}+D\nabla^4 w-L(w,\Phi)-\nabla_k\Phi+q=0 \tag{A13}$$

Letter t denotes time, whereas ρ denotes the density of the shell material. Equations (A10) and (A13) form a full system enabling the study of the movement of shallow shells when one component of displacement vector w exceeds the others. A similar situation is described as "global" buckling: the shape of the shell can change significantly under high internal momentless stresses on a large fragment of the surface. Therefore, functions w, Φ are defined within the simply connected domain S_L with boundary L, where four conditions are met:

$$w(L) = \frac{\partial w}{\partial n}(L) = 0,\ N_n(L) = \frac{\partial^2 \Phi}{\partial \alpha_s^2},\ N_s(L) = \frac{\partial^2 \Phi}{\partial \alpha_n \partial \alpha_s} \tag{A14}$$

Functions $N_n(L)$, $N_s(L)$ represent momentless stresses; n, s denote the directions of the normal and tangent, respectively, to line L.